

Half-Quantized Hall Effect at the Parity-Invariant Fermi Surface

Jin-Yu Zou, Rui Chen, Bo Fu,* Huan-Wen Wang, Zi-Ang Hu, and Shun-Qing Shen†
Department of Physics, The University of Hong Kong, Pokfulam Road, Hong Kong, China
 (Dated: September 8, 2022)

Condensed matter realization of a single Dirac cone of fermions in two dimensions is a long-standing issue. Here we report the discovery of a single gapless Dirac cone of half-quantized Hall conductance in a magnetically-doped topological insulator heterostructure. It demonstrates that the Hall conductance is half-quantized in the unit e^2/h when the parity symmetry is invariant near the Fermi surface. The gapless Dirac point is stable and protected by the local parity symmetry and the topologically nontrivial band structure of the topological insulator. The one-half Hall conductance observed in a recent experiment [Mogi et al, Nat. Phys. 18, 390 (2022)] is attributed to the existence of the gapless Dirac cone. The results suggest a condensed matter realization of a topological phase with a one-half topological invariant.

Introduction Search for a single gapless Dirac cone of fermions is a long standing issue in condensed matter physics [1–3]. In quantum field theory, an ideal massless two-dimensional Dirac fermion coupled to a U(1) gauge field gives rise to the parity anomaly, characterized by a half-quantized Hall conductance [4–8]. Lattice regularization of a single gapless Dirac cone on a lattice is not realizable if the parity symmetry is invariant according to the fermion doubling theorem [9]. One possible scheme is Wilson fermions which possess linear dispersion near the energy crossing point, but break the time reversal symmetry at higher energy [10, 11]. The proposal for the condensed matter realization of parity anomaly dates back to 1980s [12–14]. In his seminal paper [14], Haldane proposed that when one of the two valleys on a honeycomb lattice is finely tuned to be closed while another one remains open, a single flavor of massless Dirac fermion with parity anomaly can be realized. It is actually a critical transition point between a quantum anomalous Hall insulator and a conventional insulator. In graphene, the parity anomaly with half-integer quantum Hall effect is masked in view of the fourfold degeneracy from spin and valley in the system [15]. Due to the presence of the parity symmetry, the paired Dirac cones give rise to contributions to the anomaly terms with opposite signs thus exhibit no anomaly as a whole although the integer quantum Hall effect in graphene in a magnetic field has some clue of parity anomaly [16, 17]. A three-dimensional topological insulator hosts a single Dirac cone of fermions on its surface [18–21]. It provides a possible platform to observe the half-quantization of the Hall conductance, and a lot of attempts have been made in the direction [22–29]. Recently, the observation of the half-quantized Hall conductance in transport at zero magnetic field was reported as a signature of the parity anomaly in a semi-magnetic topological insulator heterostructure [30]. The paired gapless Dirac cones in a topological insulator thin film are located separately on the top and bottom surfaces. The local time reversal symmetry breaking on one surface by magnetic doping may open an energy gap for the Dirac surface

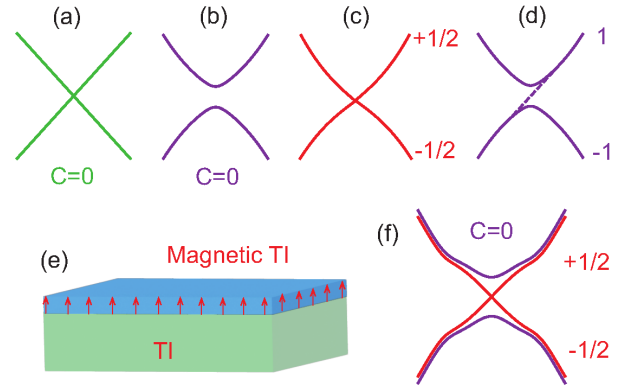


Figure 1. Four types of two-dimensional Dirac fermions and parity anomalous semimetal in a semi-magnetic topological insulator. (a) An ideal Dirac fermions with the Hall conductance $C = 0$ in the unit of $\frac{e^2}{h}$, which cannot be realized on a lattice according to the fermion doubling theorem [9]. (b) Topologically trivial gapped Dirac fermion with $C = 0$; (c) The gapless Dirac fermions of linear dispersion at the Dirac point with $C = \pm 1/2$; (d) Topologically nontrivial gapped Dirac fermion with $C = \pm 1$, i.e., Chern insulator. (e) Schematic of a semi-magnetic topological insulator film. (f) Schematic of the band structure in a semi-magnetic topological insulator, i.e., parity anomalous semimetal.

fermions while the Dirac fermions remain gapless on the other surface. Existing theories suggest that the massive Dirac fermions give rise to half-quantized Hall conductance [22, 23]. However, it is known that all the independent bands on a two-dimensional finite Brillouin zone just have an integer Chern number [31, 32]. The gapless Wilson fermions in two-dimensions have a half-quantized Hall conductance when the valence bands are fully filled [33, 34]. Thus the semi-magnetic topological insulator becomes a potential candidate to realize a single gapless Dirac cone in condensed matter.

In this Letter, we report the discovery of the gapless Dirac cone of half-quantized Hall conductance in a semi-magnetic topological insulator heterostructure. The

main results are summarized in Fig.1. The gapless Dirac cone always has one half quantized Hall conductance in the units of e^2/h when the parity symmetry is invariant near the Fermi surface. The gapless Dirac point is protected by the local parity symmetry and the topologically nontrivial band structure of the topological insulator, although the parity symmetry was broken at higher energy. The gapped Dirac cone has a nonzero Hall conductance, but becomes zero when the band is fully filled. So the massive Dirac fermions alone do not contribute a half-quantized Hall conductance to the system. The system has a minimal longitudinal conductance, and exhibits a fairly flat plateau of the half-quantized Hall conductance when Fermi level is swiping the Dirac cone. The plateau is very robust against the disorders. We term the gapless Dirac cone as parity anomalous semimetal, a semimetal with a half-quantized Hall conductance. The results suggest a condensed matter realization of the topological phase with a one-half topological invariant.

Band structure of a semi-magnetic topological insulator A semi-magnetic topological insulator film consists of topological insulator $(\text{Bi}, \text{Sb})_2\text{Te}_3$ and Cr-doped $(\text{Bi}, \text{Sb})_2\text{Te}_3$ grown by molecular-beam epitaxy. $(\text{Bi}, \text{Sb})_2\text{Te}_3$ is a topological insulator with an energy gap of about 0.3eV, and hosts a single Dirac cone of the surface electrons [35–37]. As shown in Fig. 1(e), the magnetic element Cr was doped on the top surface. The exchange interaction between the magnetic ion and the surface electrons leads to nonzero magnetization and opens an energy gap on the top surface electrons [38–41]. The Fermi energy can be finely tuned by changing the ratio of Bi and Sb such that it locates within the band gap of the top surface Dirac cone. The material has been extensively studied since the discovery of topological insulator. The topological nature of $(\text{Bi}, \text{Sb})_2\text{Te}_3$ can be well described by a tight-binding model for the electrons of $P_{z,\uparrow}$ and $P_{z,\downarrow}$ orbitals from (Bi, Sb) and Te atoms near the Fermi energy [25, 35, 42],

$$H_{TI} = \sum_i \Psi_i^\dagger \mathcal{M} \Psi_i + \sum_{i,\alpha=x,y,z} \left(\Psi_i^\dagger \mathcal{T}_\alpha \Psi_{i+\alpha} + \Psi_{i+\alpha}^\dagger \mathcal{T}_\alpha^\dagger \Psi_i \right) \quad (1)$$

where $\mathcal{M} = (m_0 - 2 \sum_\alpha t_\alpha) \sigma_0 \tau_z$, $\mathcal{T}_\alpha = t_\alpha \sigma_0 \tau_z - i \frac{\lambda_\alpha}{2} \sigma_\alpha \tau_x$, Ψ_i^\dagger and Ψ_i are the four-component creation and annihilation operators at position i . The Pauli matrices σ_α and τ_α act on the spin and orbital indices, respectively. All bands are doubly degenerate due to the coexistence of both time-reversal and inversion symmetries in the absence of magnetic doping. It can produce the linear dispersion of the surface states near the Γ point in an open boundary condition. The exchange interaction caused by Cr doping is given by a $V_{exch} = \sum_i \Psi_i^\dagger V(i) \sigma_z \tau_0 \Psi_i$ which is only present on the lattice sites of the top layers with the magnitude as V_z . In experiments, the thickness of the Cr-doped $(\text{Bi}, \text{Sb})_2\text{Te}_3$ is about 2nm and $(\text{Bi}, \text{Sb})_2\text{Te}_3$

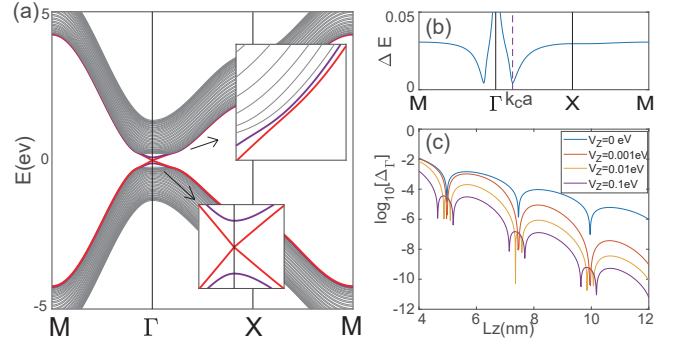


Figure 2. The band structure of a semi-magnetic topological insulator. (a) The dispersions of well separated gapless (red line) and gapped (violet line) Dirac cone in a topological insulator thin film of 8-nonmagnetic layers plus 2 magnetic-layer. Inset 1): the dispersions near the Γ point; Inset 2): the anti-band crossing point between the gapless and gapped Dirac cones. (b) The energy separation between the gapless and gapped Dirac cones. (c) The energy difference of the gapless Dirac cone at the Γ point as a function of the thickness L_z for several values of exchange interaction V_z on the top layer. Model parameters: $\lambda_x = \lambda_y = \lambda_{\parallel} = 0.41$ eV, $\lambda_z = \lambda_{\perp} = 0.44$ eV, and $t_x = t_y = t_{\parallel} = 0.566$ eV, $t_z = t_{\perp} = 0.40$ eV and $m_0 = 0.28$ eV. $V_z = 0.1$ eV if with no specific indication.

layer is about 8nm [30]. We take the periodic boundary condition in the x- and y-direction and open boundary condition in the z direction, the calculated dispersions are presented in Fig. 2a. It is noted that there exist a gapless Dirac cone and a gapped Dirac cone within the bulk gap. The dispersions for the gapless Dirac cone cross at the Γ point and are linear in k around the crossing point. The gapped Dirac cone opens an energy gap of about $2V_z$, which is caused by the exchange interaction of Cr-doping on the top surface. Numerical calculation shows that the gapless and gapped states within the bulk band gap are mainly located on the bottom and top surfaces, respectively. We check the energy separation between the two bands along the high symmetric lines, and find that the gapless Dirac cone and gapped Dirac cone are well separated. The dip at k_c indicates that there exists a band mixture. Finite thickness of the film may cause a tiny gap at the Γ point, which decays exponentially in the thickness approximately [43, 44]. With increasing exchange interaction, the gap is quickly suppressed by several order of magnitude to negligibly small (about 10^{-10} eV. for a thickness $L_z = 10$ nm, see Fig. 2c). It will be smeared out easily by temperature broadening ($1K$ is about $0.086 meV$) in experimental measurements.

The Hall conductance and the Berry curvature Using the Kubo formula for the electric conductivity [45], we calculate the Hall conductance as a function of the chemical potential μ_F numerically for the tight-binding model in Eq. 1 with a thickness $L_z = 10$ nm. A fairly flat plateau of $-\frac{e^2}{2h}$ appears within the band gap as shown in Fig. 3a. To figure out the origin of the conductance

plateau, we first note that there exists a full band gap between four lowest energy bands and the rest at all k . These four bands form well-separated band-subspaces and the Hall conductance as a function of μ_F can be calculated for each band. We then only focus on the gapless and gapped Dirac cones denoted by red and violet lines in Fig. 2a. For the gapped Dirac cone, we have a nonzero Hall conductance as μ_F varies, which has its maximal about $0.4\frac{e^2}{h}$, but decays to zero quickly when the band is fully occupied. The maximal value may increase for a thicker film, but always be lower than $0.5\frac{e^2}{h}$. This is consistent with the fact that the Chern number of a well-defined band in a finite Brillouin zone is always an integer (including zero) [21, 32]. For the gapless Dirac cone, the Hall conductance becomes $-0.5\frac{e^2}{h}$ within the bulk band gap, which is larger than the gap of the gapped Dirac cone. Thus the total Hall conductance within the bulk band gap are mainly contributed by these two bands and the Hall conductance plateau is attributed to the gapless Dirac cone instead of the gapped Dirac cone.

To explore the topological nature of the gapless Dirac cone and its relation to the Hall conductance, we studied the Berry curvature of the gapless bands. In the Bloch states $|u_{n,\mathbf{k}}\rangle$, the Berry connection and the Berry curvature are defined as $\mathcal{A}_{n,\alpha}(\mathbf{k}) = i\langle u_{n,\mathbf{k}}|\partial_{k_\alpha}u_{n,\mathbf{k}}\rangle$ and $\Omega_z^n(\mathbf{k}) = \partial_{k_x}\mathcal{A}_{n,y}(\mathbf{k}) - \partial_{k_y}\mathcal{A}_{n,x}(\mathbf{k})$, respectively [32]. For the gapless Dirac cone, it is found that the Berry curvature $\Omega_z^n(\mathbf{k}) = 0$ within the regime of $k < k_c$. Beyond the regime, it becomes negative and finally vanishes for a larger k . Combining with the band structure, the nonzero Berry curvature mainly originates from hybridization of the states from the top and bottom layers. The conductance plateau appears when the chemical potential is located in the regime where the Berry curvature vanishes.

On the parity-invariant regime Now we come to discuss the origin of the parity-invariant regime based on the tight-banding model in Eq. (1). For each wave vector \mathbf{k} , the Hamiltonian can be divided into two parts, $H_{TI}(\mathbf{k}) = H_{1d}(\mathbf{k}) + H_S(\mathbf{k})$. H_{1d} is equivalent to a one-dimensional lattice model with a gap $m_0(k) = m_0 - 4t_{\parallel} \left(\sin^2 \frac{k_x a}{2} + \sin^2 \frac{k_y a}{2} \right)$ [21],

$$H_{1d}(\mathbf{k}) = \sum_{i_z} \left(\Psi_{i_z, \mathbf{k}}^\dagger \mathcal{M}(\mathbf{k}) \Psi_{i_z, \mathbf{k}} + \Psi_{i_z, \mathbf{k}}^\dagger \mathcal{T}_z \Psi_{i_z+1, \mathbf{k}} + h.c. \right) \quad (2)$$

with $\mathcal{M}(\mathbf{k}) = [m_0(k) - 2t_{\perp}] \sigma_0 \tau_z$, and $H_S(\mathbf{k}) = \lambda_{\parallel} \sum_{i_z, \alpha=x,y} \Psi_{i_z, \mathbf{k}}^\dagger \sin(k_\alpha a) \sigma_\alpha \tau_x \Psi_{i_z, \mathbf{k}}$. For $m_0(k) > 0$, *i.e.* $k < k_c \simeq \sqrt{M/t_{\parallel}}/a$, H_{1d} is topologically non-trivial. There exist a pair of zero energy modes at each side or near the top surface and bottom surface. Denote ξ_s and χ_t the two eigenvectors of σ_z and τ_y with eigen values $s = \pm 1$ and $t = \pm 1$. The zero energy modes are the eigen vectors $\xi_s \otimes \chi_t$ of the operator $\sigma_z \tau_y$ with the eigenvalue $S = st$. The spatial part of the two states of $S = 1$ ($s = t = 1$ and $s = t = -1$) are

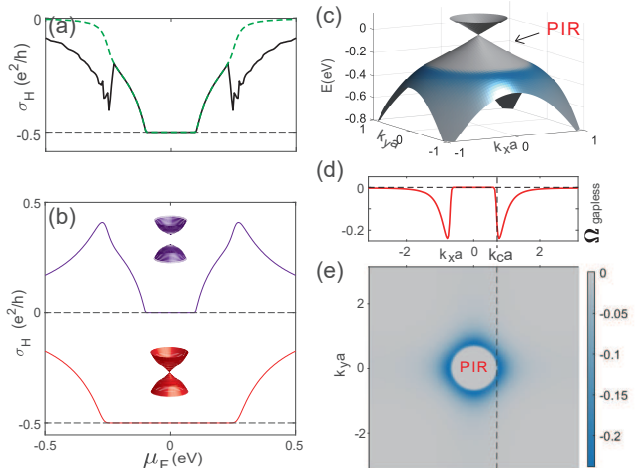


Figure 3. (a) The Hall conductance as a function of the chemical potential μ_F for the thin film. The green dashed line is the combination of the Hall conductance of the gapless and gapped Dirac cones. (b) The Hall conductance of the gapless and gapped Dirac cones. (c) The gapless Dirac cone in a two-dimensional Brillouin zone. The color indicates the value of the Berry curvature of the states. (d) The Berry curvature of the gapless valence band as a function of k_x ($k_y = 0$). (e) The Berry curvature and the parity-invariant regime (PIR) in the Brillouin zone.

mainly located near the top surface and the two states of $S = -1$ are located near the top surface, and decay exponentially to its opposite side [21]. By mapping $H_S(\mathbf{k}) + V_{exch}$ into the basis of the four states, one obtains the effective Hamiltonian of the gapless Dirac cone $H_b(k) = -\lambda_{\parallel} (\sin(k_x a) \sigma_y - \sin(k_y a) \sigma_x)$ which is mainly located at the bottom layer and the gapped Dirac cone $H_t(k) = +\lambda_{\parallel} (\sin(k_x a) \sigma_y - \sin(k_y a) \sigma_x) + V(k) \sigma_z$ which is at the top layer. $V(k)$ is given by the expectation of the exchange interaction V_{exch} , and varies with the wave vector, especially when $m_0(k) \rightarrow 0$ where the wave function of zero energy modes evolve to distribute broadly in space. In two dimensions, the parity symmetry is defined by $\mathcal{P}H(\mathbf{k})\mathcal{P}^{-1} = H(\hat{M}\mathbf{k})$, where $\mathcal{P} = i\sigma_y$ and \hat{M} is the mirror operator in momentum space transforming $\mathbf{k} \rightarrow \hat{M}\mathbf{k} = (k_x, -k_y)$. Thus in the regime the gapless Dirac cone $\mathcal{P}H_b(\mathbf{k})\mathcal{P}^{-1} = H_b(\hat{M}\mathbf{k})$ respects the parity symmetry while the gapped Dirac cone $\mathcal{P}H_t(\mathbf{k})\mathcal{P}^{-1} \neq H_t(\hat{M}\mathbf{k})$ breaks the symmetry due to the presence of $V(k)$. Thus the nontrivial condition of $m_0(k) > 0$ defines a parity-invariant regime for the gapless Dirac cone. In addition to the local parity symmetry, H_b also respects a space-time operator $I_{ST} = C_{2z}T$ where C_{2z} is a twofold rotation about the z axis, and T is local time reversal operator. $I_{ST}^2 = +1$ imposes a further constraint on the Berry curvature, leading to $\Omega_z^n(\mathbf{k}) = 0$. When $m_0(k) < 0$, H_{1d} becomes topologically trivial. The zero energy modes evolve into the bulk states with nonzero energy. The states are no longer the

eigen-vectors of the operator $\sigma_z \tau_y$, and break the parity symmetry. Based on this picture, we propose an effective four-band model

$$H_F = \lambda_{||}(\sin k_x a \sigma_y - \sin k_y a \sigma_x) \gamma_z + V(k) \sigma_z (\gamma_z + 1) + H_{\Delta}^{\text{eff}} \quad (3)$$

where $H_{\Delta}^{\text{eff}} = f(k) m_0(k) \gamma_x$ describes the hybridization of the states. A Fermi-Dirac-distribution-like factor or the sigmoid function $f(k) = \left[\exp\left(\frac{m_0(k)}{T^*}\right) + 1 \right]^{-1}$ is introduced to describe the procedure that the coupling is eventually turned on at higher energy. $\gamma_{x,z}$ are the Pauli matrices representing the top and bottom layers. A small T^* is a model-specific parameter. The calculated results show that the model can reproduce the key features of the band structure. The Hall conductance as a function of μ_F is given by $\sigma_H^S = \frac{e^2}{2h}(S - \cos \phi_S(k_F^S))$. The part of S is mainly attributed to the hybridization term H_{Δ}^{eff} and the band splitting $V(k)$. For the gapless band of $S = -1$, $\cos \phi_S(k_F^S) = 0$ in the parity-invariant regime and $\sigma_H^{-1} = -\frac{e^2}{2h}$. For the gapped band of $S = +1$, $\cos \phi_S = 1$ for the full occupancy and $\sigma_H^{+1} = 0$. They are in a good agreement with the numerical results in Fig. 3b. The details are referred to Ref. [47].

Half-quantization and parity symmetry Now we present a relation between the half-quantization of the Hall conductance and the parity symmetry. In the Haldane model and the Wilson fermions, it was found that the Hall conductance is half-quantized when the chemical potential is located at the energy crossing point [14, 33]. Here we prove that the Hall conductance is one half of an integer if the parity symmetry is respected near the Fermi level μ_F . In two dimensions, the intrinsic Hall conductance for band n can be expressed in terms of the Berry gauge field in momentum space [32],

$$\sigma_H^n(\mu_F) = \frac{e^2}{h} \int \frac{d^2 k}{2\pi} \epsilon^{ij} \partial_{k_i} \mathcal{A}_{n,j} \theta(\varepsilon_{n,\mathbf{k}} - \mu_F) \quad (4)$$

where $\theta(x)$ is the step function, *i.e.*, $\theta(x) = 1$ for $x \leq 0$ and zero otherwise. The whole Brillouin zone can be divided into two patches by the Fermi level μ_F , the occupied and unoccupied regime, respectively. By using the Stokes' theorem, the integral of the Berry curvature over the occupied regime can be converted into the integrals over the Fermi surface (FS), $\sigma_H^n(\mu_F) = \frac{e^2}{h} \frac{1}{2\pi} \oint_{FS} d\vec{l}_F \cdot \vec{\mathcal{A}}_n$, where \vec{l}_F is the wave vector along the Fermi surface. Consider the case that the Hamiltonian $H(\mathbf{k})$ is invariant under the parity symmetry along the Fermi surface, *i.e.* $\mathcal{P}H(\mathbf{k})\mathcal{P}^{-1} = H(\hat{M}\mathbf{k})$. The eigenstates of $H(\mathbf{k})$ at \mathbf{k} and $\hat{M}\mathbf{k}$ on the Fermi edge must be related by a gauge transformation: $\mathcal{P}|u_n(\mathbf{k})\rangle = \exp[i\theta_n(\mathbf{k})]|u_n(\hat{M}\mathbf{k})\rangle$. Accordingly, the Berry connection is transformed to $\mathcal{A}_{n,i}(\mathbf{k}) = \partial_{k_i} \theta_n(\mathbf{k}) + \sum_j J_{ij} \mathcal{A}_{n,j}(\hat{M}\mathbf{k})$ with $J_{ab} = \partial(\hat{M}\mathbf{k})_b / \partial k_a$. The determinant of the Jacobian matrix J_{ab} equals -1 . It follows that $2\sigma_H^n = \frac{e^2}{h} \frac{1}{2\pi} \oint_{FS} d\vec{l}_F \cdot \nabla_{\vec{l}_F} \theta_n(\mathbf{k}) = \frac{e^2}{h} \nu$. For

a linear dispersion near the Dirac point, the Berry phase around the Fermi surface is $+\pi$ or $-\pi$, depending on the helicity of the Dirac fermions. Correspondingly ν is equal to $+1$ or -1 . Thus the Hall conductance $\sigma_H = \frac{\nu}{2} \frac{e^2}{h}$ is half quantized in the case that the parity symmetry is restored near the Fermi level.

Disorders and robustness of the quantized Hall conductance The robustness of the half-quantized Hall conductance comes from two aspects. One is the local parity invariance for the gapless Dirac cone. The exchange interaction is only present at the top surface. The low-energy dispersion of the gapless Dirac cone is mainly located at the bottom layer, and is less affected by the exchange interaction, although the part of higher energy is modified. The other aspect is that the presence of the surface states is mainly attributed to the three-dimensional band structure of the topological insulator. It is known that the topology of the band structure of three-dimensional topological insulator is very robust against the disorders. If the strength of disorders is not strong enough to induce a topological phase transition, the gapless surface states are still present. In this way the Dirac point is very stable against the disorders before the phase transition occurs.

To illustrate the robustness of the single Dirac cone in this quasi-two-dimensional system, we calculated the Hall conductance as a function of the strength of disorders. We follow the common practice in the study of Anderson localization to introduce disorder through random non-magnetic on-site energy with a uniform distribution with $[-W/2, +W/2]$. We calculate the Hall conductance of a disordered square of size $L_x \times L_y \times L_z$ for a fixed thickness L_z by means of the noncommutative Kubo formula [49]

$$\sigma_H = i2\pi \text{Tr} \{ \mathbf{P} [-i[\mathbf{x}, \mathbf{P}], -i[\mathbf{y}, \mathbf{P}]] \} \frac{e^2}{h} \quad (5)$$

with the periodic boundary conditions along the x and y directions. Here, \mathbf{x} and \mathbf{y} are the coordinate operators and $\text{Tr}\{\dots\}$ is the trace over the occupied bands. \mathbf{P} is the projector onto the occupied states of the system. Figure 4 shows the numerically calculated disorder-averaged Hall conductances as functions of the disorder strength. In the clean limit, the system exhibits the half-quantized Hall conductance as expected. With increasing disorder strength, the Hall conductance remains about $0.5 \frac{e^2}{h}$ until the disorder strength W exceeds about 0.83eV . The critical disorder strength is much larger than the exchange interaction and also larger than the bulk energy gap of topological insulator. Further increasing the disorder strength, the conductance drops quickly and the system is expected to be localized by disorders. Thus, the half-quantized Hall conductance is robust against the disorder. This demonstrates explicitly that the gapless Dirac cone is quite stable against the disorders.

The presence of impurities will cause the scattering between electron wave functions which leads to an energy level repulsion effect[50]. The stability of the Dirac point

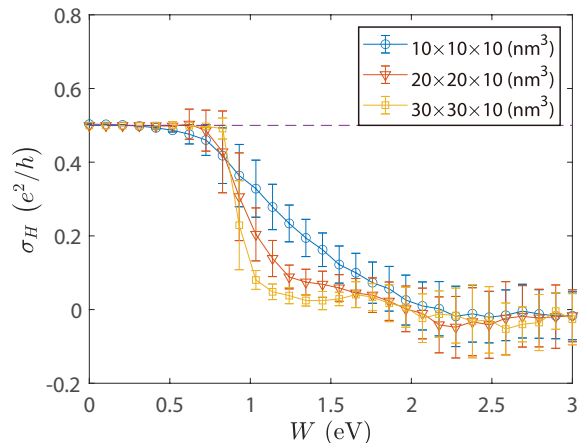


Figure 4. The Hall conductance as a function of the strength of nonmagnetic disorders $U_i\sigma_0\tau_0$ for several lattice sizes $L_x \times L_y \times L_z$ for a fixed $L_z = 10\text{nm}$. The Fermi level $\mu_F = 0.01\text{ eV}$ and the lattice spacing $a = 1\text{nm}$. 200 random configurations are adopted to average for each value.

is thus equivalent to examine the relative energy level repulsion between the two states at Dirac point from all other surface and bulk states. The scatterings between two bottom surface states will not introduce Dirac mass renormalization due to the presence of the local time reversal symmetry. The scatterings from the top surface states can also be neglected due to the fact that the two opposite surface states have exponentially small overlap. The magnetic doping on the top surface will cause an energy splitting $\sim V_z L_z^{\text{mag}}/L_z$ for the two degenerate bulk states with L_z^{mag} as the thickness of the magnetic layers. For sufficiently small L_z^{mag}/L_z , the energy level repulsion effect from two nearly degenerate bulk states will be cancelled out. This picture is verified by a self-energy calculation in the self-consistent Born approximation based on the effective four-band model [47]. Compared with the two-band model[51], the contributions to the Dirac mass renormalization from the gapped and gapless bands in the four-band model alternate in sign and cancel each other out at high energy. As a consequence, the Dirac point is still stable even in the presence of disorder due to the local time-reversal symmetry, and the accompanying gapped bands.

The authors would like to thank Junren Shi and Qian Niu for helpful discussions. The numerical calculations were supported by Center for Computational Science and Engineering of SUSTech. This work was supported by the Research Grants Council, University Grants Committee, Hong Kong under Grant Nos. C7012-21G and 17301220 and the National Key R&D Program of China under Grant No. 2019YFA0308603.

* fubo@hku.hk

† sshen@hku.hk

- [1] S. Murakami, Phase transition between the quantum spin Hall and insulator phases in 3D: emergence of a topological gapless phase. *New J. Phys.* **9**, 356 (2007).
- [2] B. J. Yang, and N. Nagaosa, Classification of stable three-dimensional Dirac semimetals with nontrivial topology. *Nat. Commun.* **5**, 4898 (2014).
- [3] N. P. Armitage, E. J. Mele, and A. Vishwanath, Weyl and Dirac semimetals in three-dimensional solids. *Rev. Mod. Phys.* **90**, 015001 (2018).
- [4] A. J. Niemi and G. W. Semenoff, Axial-anomaly-induced fermion fractionization and effective gauge-theory actions in odd-dimensional space-times, *Phys. Rev. Lett.* **51**, 2077 (1983).
- [5] R. Jackiw, Fractional charge and zero modes for planar systems in a magnetic field, *Phys. Rev. D* **29**, 2375 (1984).
- [6] A. N. Redlich, Gauge noninvariance and parity nonconservation of three-dimensional fermions. *Phys. Rev. Lett.* **52**, 18–21 (1984).
- [7] D. Boyanovsky, R. Blankenbecler, and R. Yahalom, Physical origin of topological mass in 2+ 1 dimensions, *Nucl. Phys. B* **270**, 483 (1986).
- [8] A. M. J. Schakel, Relativistic quantum Hall effect, *Phys. Rev. D* **43**, 1428 (1991).
- [9] H. B. Nielsen, and M. Ninomiya, A no-go theorem for regularizing chiral fermions, *Phys. Lett.* **105B**, 219 (1981).
- [10] K. G. Wilson, *New Phenomena in Subnuclear Physics*, ed. A. Zichichi (New York, Plenum, 1975).
- [11] H. J. Rothe, *Lattice gauge theories: an introduction*, 3rd ed. (World Scientific, Singapore, 2005).
- [12] G. W. Semenoff, Condensed-Matter Simulation of a Three-Dimensional Anomaly, *Phys. Rev. Lett.* **53**, 2449 (1984).
- [13] E. Fradkin, E. Dagotto, and D. Boyanovsky, Physical Realization of the Parity Anomaly in Condensed Matter Physics, *Phys. Rev. Lett.* **57**, 2967 (1986).
- [14] F. D. M. Haldane, Model for a Quantum Hall Effect without Landau Levels: Condensed-Matter Realization of the "Parity Anomaly", *Phys. Rev. Lett.* **61**, 2015 (1988).
- [15] A. H. Castro Neto, F. Guinea, N. M. R. Peres, K. S. Novoselov, and A. K. Geim, The electronic properties of graphene. *Rev. Mod. Phys.* **81**, 109 (2009).
- [16] K. S. Novoselov, A. K. Geim, S. V. Morozov, D. Jiang, M. I. Katsnelson, I. V. Grigorieva, S. V. Dubonos, and A. A. Firsov, Two-dimensional gas of massless Dirac fermions in graphene, *Nature* **438**, 197 (2005).
- [17] Y. B. Zhang, Y. W. Tan, H. L. Stormer, and P. Kim, Experimental observation of the quantum Hall effect and Berry's phase in graphene, *Nature* **438**, 201 (2005).
- [18] L. Fu, C. L. Kane, and E. J. Mele, Topological insulators in three dimensions, *Phys. Rev. Lett.* **98**, 106803 (2007).
- [19] M. Z. Hasan, and C. L. Kane, Colloquium: topological insulators, *Rev. Mod. Phys.* **82**, 3045 (2010).
- [20] X. L. Qi, and S. C. Zhang, Topological insulators and superconductors, *Rev. Mod. Phys.* **83**, 1057 (2011)
- [21] S. Q. Shen, *Topological insulators*, Springer Series of Solid State Science, Vol. 174 (Springer, Heidelberg, 2012).
- [22] L. Fu and C. L. Kane, Topological insulators with inversion symmetry. *Phys. Rev. B* **76**, 045302 (2007).

- [23] X. L. Qi, T. L. Hughes, and S. C. Zhang, Topological field theory of time-reversal invariant insulators. *Phys. Rev. B* **78**, 195424 (2008).
- [24] A. M. Essin, J. E. Moore, and D. Vanderbilt, Magneto-electric polarizability and axion electrodynamics in crystalline insulators. *Phys. Rev. Lett.* **102**, 146805 (2009).
- [25] R. L. Chu, J. R. Shi, and S. Q. Shen, Surface edge state and half-quantized Hall conductance in topological insulators. *Phys. Rev. B* **84**, 085312 (2011).
- [26] E. J. Koenig, P. M. Ostrovsky, I. V. Protopopov, I. V. Gornyi, I. S. Burmistrov, and A. D. Mirlin, Half-integer quantum Hall effect of disordered Dirac fermions at a topological insulator surface. *Phys. Rev. B* **90**, 165435 (2014).
- [27] Y. Xu, I. Miotkowski, C. Liu, J. Tian, H. Nam, N. Alidoust, J. Hu, C. K. Shih, M. Z. Hasan & Y. P. Chen, Observation of topological surface state quantum Hall effect in an intrinsic three-dimensional topological insulator. *Nat. Phys.* **10**, 956 (2014).
- [28] S. Zhang, L. Pi, R. Wang, G. Yu, X. -C. Pan, Z. Wei, J. Zhang, C. Xi, Z. Bai, F. Fei, M. Wang, J. Liao, Y. Li, X. Wang, F. Song, Y. Zhang, B. Wang, D. Xing and G. Wang, Anomalous quantization trajectory and parity anomaly in Co cluster decorated BiSbTeSe₂ nanodevices, *Nat. Commun.* **8**, 977 (2017).
- [29] J. Böttcher, C. Tutschku, L. W. Molenkamp, and E. M. Hankiewicz, Survival of the Quantum Anomalous Hall Effect in Orbital Magnetic Fields as a Consequence of the Parity Anomaly, *Phys. Rev. Lett.* **123**, 226602 (2019).
- [30] M. Mogi, Y. Okamura, M. Kawamura, R. Yoshimi, K. Yasuda, A. Tsukazaki, K. S. Takahashi, T. Morimoto, N. Nagaosa, M. Kawasaki, Y. Takahashi, and Y. Tokura, Experimental signature of parity anomaly in semi-magnetic topological insulator, *Nat. Phys.* **18**, 390 (2022).
- [31] D. J. Thouless, M. Kohmoto, M. P. Nightingale, and M. den Nijs, Quantized Hall Conductance in a Two-Dimensional Periodic Potential. *Phys. Rev. Lett.* **49**, 405 (1982).
- [32] D. Xiao, M. C. Chang, Q. Niu, Berry phase effects on electronic properties. *Rev. Mod. Phys.* **82**, 1959 (2010).
- [33] B. Fu, J. Y. Zou, Z. A. Hu, H. W. Wang, and S. Q. Shen, Quantum anomalous semimetals. To appear in *npj Quantum Mater.* (2022), arXiv:2203.00933.
- [34] J. Y. Zou, B. Fu, H. W. Wang, Z. A. Hu, S. Q. Shen, Half-quantized Hall effect and power law decay of edge-current distribution, *Phys. Rev. B* **105**, L201106 (2022).
- [35] H. Zhang, C. X. Liu, X. L. Qi, X. Dai, Z. Fang, and S. C. Zhang, Topological insulators in Bi₂Se₃, Bi₂Te₃ and Sb₂Te₃ with a single Dirac cone on the surface. *Nat. Phys.* **5**, 438 (2009)
- [36] Y. Xia, D. Qian, D. Hsieh, L. Wray, A. Pal, H. Lin, A. Bansil, D. Grauer, Y. S. Hor, R. J. Cava & M. Z. Hasan, Observation of a large-gap topological-insulator class with a single Dirac cone on the surface. *Nat. Phys.* **5**, 398 (2009).
- [37] Y. L. Chen, J. G. Analytis, J.-H. Chu, Z. K. Liu, S.-K. Mo, X. L. Qi, H. J. Zhang, D. H. Lu, X. Dai, Z. Fang, S. C. Zhang, I. R. Fisher, Z. Hussain, and Z.-X. Shen, Experimental Realization of a Three-Dimensional Topological Insulator, Bi₂Te₃. *Science* **325**, 178 (2009).
- [38] R. Yu, W. Zhang, H. J. Zhang, S. C. Zhang, X. Dai, and Z. Fang, Quantized anomalous Hall effect in magnetic topological insulators. *Science* **329**, 61 (2010).
- [39] Y. L. Chen, J. H. Chu, J. G. Analytis, Z. K. Liu, K. Igarashi, H. H. Kuo, X. L. Qi, S. K. Mo, R. G. Moore, D. H. Lu, M. Hashimoto, T. Sasagawa, S. C. Zhang, I. R. Fisher, Z. Hussain, and Z. X. Shen Massive Dirac fermion on the surface of a magnetically doped topological insulator. *Science* **329**, 659 (2010).
- [40] C. Z. Chang, J. Zhang, X. Feng, J. Shen, Z. Zhang, M. Guo, K. Li, Y. Ou, P. Wei, L. L. Wang, Z. Q. Ji, Y. Feng, S. Ji, X. Chen, J. Jia, X. Dai, Z. Fang, S. C. Zhang, K. He, Y. Wang, L. Lu, X. C. Ma, and Q. K. Xue, Experimental observation of the quantum anomalous Hall effect in a magnetic topological insulator. *Science* **340**, 167–170 (2013).
- [41] R. Yoshimi, K. Yasuda, A. Tsukazaki, K. S. Takahashi, N. Nagaosa, M. Kawasaki and Y. Tokura, Quantum Hall states stabilized in semi-magnetic bilayers of topological insulators. *Nat. Commun.* **6**, 8530 (2015).
- [42] C. X. Liu, X. L. Qi, H. J. Zhang, X. Dai, Z. Fang, and S. C. Zhang, Model Hamiltonian for topological insulators, *Phys. Rev. B* **82**, 045122 (2010).
- [43] H. Z. Lu, W. Y. Shan, W. Yao, Q. Niu, and S. Q. Shen. Massive Dirac fermions and spin physics in an ultrathin film of topological insulator. *Phys. Rev. B* **81**, 115407 (2010).
- [44] J. Linder, T. Yokoyama, and A. Sudbø, Anomalous finite size effects on surface states in the topological insulator Bi₂Se₃. *Phys. Rev. B* **80**, 205401 (2009)
- [45] G. D. Mahan, *Many-Particle Physics*, (Springer, New York, 2000).
- [46] Y. Zhang, K. He, C. Z. Chang, C. L. Song, L. Wang, X. Chen, J. Jia, Z. Fang, X. Dai, W. Y. Shan, S. Q. Shen, Q. Niu, X. L. Qi, S. C. Zhang, X. C. Ma, Q. K. Xue, Crossover of three-dimensional topological insulator of Bi₂Se₃ to the two-dimensional limit. *Nat. Phys.* **6**, 584 (2010).
- [47] See Supplemental Material at [URL to be added by publisher] for details of (Sec. SI)The model Hamiltonian, (Sec. SII) the zero modes, (Sec. SIV) the robustness of the Hall conductance in the presence of disorder, and (Sec. V) the precision of half-quantized Hall plateau, which includes Refs.([11, 21, 35, 45, 46, 48, 51]).
- [48] H. Haug and A.-P. Jauho, *Quantum kinetics in transport and optics of semiconductors* (Springer-Verlag, Berlin, 1996).
- [49] E. Prodan, Disordered topological insulators: a non-commutative geometry perspective. *J. Phys. A: Math. Theor.* **44**, 113001 (2011).
- [50] C. W. J. Beenakker, Random-matrix theory of quantum transport, *Rev. Mod. Phys.* **69**, 731 (1997).
- [51] C. W. Groth, M. Wimmer, A. R. Akhmerov, J. Tworzydło, and C. W. J. Beenakker, Theory of the topological Anderson insulator. *Phys. Rev. Lett.* **103**, 196805 (2009)